Structure-Based Mutational Analysis of the 4′-Phosphopantetheinyl Transferases Sfp from *Bacillus subtilis*: Carrier Protein Recognition and Reaction Mechanism[†,‡]

Mohammad Reza Mofid, Robert Finking, Lars Oliver Essen, and Mohamed A. Marahiel*

Fachbereich Chemie/Biochemie, Philipps-Universität Marburg, Hans-Meerwein-Strasse, D-35032 Marburg, Germany

Received November 11, 2003; Revised Manuscript Received February 5, 2004

ABSTRACT: The activation of apo-peptidyl carrier proteins (PCPs) of nonribosomal peptide synthetases (NRPSs), apo-acyl carrier proteins (ACPs) of polyketide synthases (PKSs), and fatty acid synthases (FASs) to their active holo form is accomplished with dedicated 4′-phosphopantetheinyl transferases (PPTases). They catalyze the transfer of the essential prosthetic group 4′-phosphopantetheine (4′-Ppant) from coenzyme A (CoA) to a highly conserved serine residue in all PCPs and ACPs. PPTases, based on sequence and substrate specifity, have been classified into three types: bacterial holo-acyl carrier protein synthase (AcpS), fatty acid synthase of eukaryotes (FAS2) and Sfp, a PPTase of secondary metabolism. The recently solved crystal structures of AcpS and Sfp-type PPTases with CoA revealed a common $\alpha + \beta$-fold with a $\beta_1\alpha_3\beta_2$ motif and similarities in CoA binding and polymerization mode. However, it was not possible to discern neither the PCP binding region of Sfp nor the priming reaction mechanism from the Sfp−CoA cocrystal. In this work, we provide a model for the reaction mechanism based on mutational analysis of Sfp that suggests a reaction mechanism in which the highly conserved E151 deprotonates the hydroxyl group of the invariant serine of PCP. That, in turn, acts as a nucleophile to attack the β-phosphate of CoA. The Sfp mutants K112, E117, and K120 further revealed that the loop region between $\beta 4$ and $\alpha 5$ (residues T111−S124) in Sfp is the PCP binding region. Also, residues T44, K75, S89, H90, D107, E109, E151, and K155 that have been shown in the Sfp−CoA cocrystal structure to coordinate CoA are now all confirmed by mutational and biochemical analysis.

The 4′-phosphopantetheinyl moiety (4′-Ppant)[1] plays an essential role as a cofactor of multienzyme complexes such as nonribosomal peptide synthetases (NRPSs), polyketide synthases (PKSs), and fatty acid synthases (FASs) (*1−4*). FASs are responsible for the biosynthesis of fatty acids and are therefore part of the primary metabolism. NRPSs and PKSs, on the other hand, produce a diverse number of natural products that are part of the secondary metabolism, e.g., the peptide antibiotic vancomycin or the immunosuppressive agent cyclosporin (*5, 6*). The mobile 4′-Ppant prosthetic group is about 20 Å in length and is covalently bound as a phosphodiester to an invariant serine residue of a carrier protein domain which is part of the multienzyme complex. These carrier proteins (CPs) are small proteins of 8−10 kDa and exist either as a distinct protein (type II) or as integrated domains of larger polypeptide chains (type I). CPs play an essential role because they transfer the 4′-Ppant-bound substrate or intermediates to different catalytic centers of the multienzyme complex. Because of differences in the substrate bound, CPs have been named acyl carrier protein (ACP), aryl carrier protein (ArCP), or peptidyl carrier protein (PCP).

The transfer of 4′-Ppant onto the carrier protein is catalyzed by a dedicated 4′-phosphopantetheinyl transferase (PPTase, EC 2.7.8.7) (*7*). The PPTase converts inactive apo-carrier protein to the functionally active holo form. This reaction involves the nucleophilic attack of the hydroxyl side chain of the highly conserved serine residue of the carrier protein on the 5′-β-phosphate of CoA, thereby releasing 3′,5′-ADP (Figure 1).

This posttranslational modification is essential for the activity of the multienzyme complex (*8, 9*). Earlier analysis of *Bacillus subtilis* JH642 has shown that, although the strain harbors the intact surfactin synthetase, it did not produce the lipopeptide surfactin as a result of a truncated *sfp* gene (495 bp) that encodes the dysfunctional Sfp PPTase (*10*). However, if *B. subtilis* JH642 is provided with an intact copy of the *sfp* gene (672 bp), it produces the lipoheptapeptide surfactin.

The use of CPs as the carriers of activated intermediates is not restricted to the above-mentioned pathways. Other examples of biosynthetic pathways that make use of this strategy include lysine biosynthesis in yeast, D-alanylation of the lipoteichoic acid in the cell wall of *B. subtilis* and *Lactobacillus casei*, or oligosaccharide nodulation (*11−13*). Genes encoding PPTases are frequently associated with the gene clusters encoding the corresponding multienzymes. For instance, *sfp* is located 4 kbp downstream of the surfactin
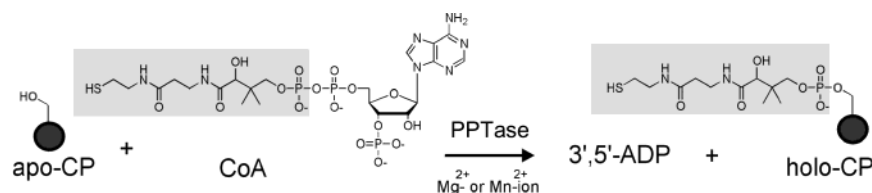
FIGURE 1: Priming reaction in NRPS by Sfp. Sfp converts CPs, in the presence of Mg^{2+} or Mn^{2+} ions, from their inactive apo form to the active holo form by transfer of a 4′-phosphopantetheinyl moiety from coenzyme A onto the hydroxyl side chain of a conserved serine residue of the CP.

synthase gene cluster, *mtaA* is a direct neighbor of the gene cluster encoding myxothiazol synthase, and the cytoplasmic PPTase from *Saccharomyces cerevisiae* is an integrated domain of FAS2 (*14, 15*).

Biochemical characterization of different PPTases from a variety of organisms has unveiled a certain pattern that allows classification of PPTases into three groups based on their primary sequence and substrate specificity (*7*). The first group comprises bacterial holo-acyl carrier protein synthase (AcpS) that is about 120−140 amino acids in size (*16*). AcpS-type PPTases are associated with fatty acid synthase (FAS) of prokaryotes and accept only the ACP of FAS and ACPs of type II PKSs. The second group is named after a PPTase of fatty acid synthase in eukaryotes (FAS2) that are integrated domains of FAS in eukaryotes, e.g., in *S. cerevisiae* (*15*). The PPTase domain of FAS2 is about 120 amino acids in size and accepts only the ACP of the multienzyme complex FAS in eukaryotes. Sfp, a PPTase of secondary metabolism, accepts a wide range of carrier protein substrates and is about twice the size of an AcpS-type PPTase (220−240 amino acids) (*17*). Sfp is the classic example of type 3 PPTases. Although these PPTases are usually associated with secondary metabolism (i.e., NRPS and PKS pathways), some organisms rely on this type of enzyme as the only PPTase present (*18*).

The recently solved crystal structures of PPTases from the AcpS and Sfp groups have yielded detailed insight into the interaction between the enzymes and their substrates (*19, 20*). However, it was not possible to discern neither the reaction mechanism based on the cocrystal of Sfp with CoA nor the PCP binding region in Sfp. AcpS of *B. subtilis*, on the other hand, was crystallized in the presence of its cognate protein partner, ACP. In this study, we present in vitro analysis of Sfp mutants generated by site-directed mutagenesis. As we will show, these mutants allow the proposal of a catalytic mechanism of PPTases for the posttranslational modification of PCP and the mode of substrate recognition as well as the PCP and CoA binding sites of Sfp.

EXPERIMENTAL PROCEDURES

General Techniques. Escherichia coli was grown on LB medium. Ampicillin was used at 100 μg/mL concentration. For *E. coli* techniques, such as transformation and plasmid preparation, standard protocols were used (*21*). Oligonucleotides were purchased from Qiagen-Operon (Cologne, Germany). [^{3}H]CoA was purchased from Hartmann Analytics (Braunschweig, Germany).

Mutagenesis of the sfp Gene. Mutations in the *sfp* genes were introduced by one of two methods:

The QuickChange kit (Stratagene, Heidelberg, Germany) was applied according to the manufacturer's recommenda-

tions (method A) using two primers with the desired mutation in a PCR with pQE60-*sfp* (*22*) as template and *Pfu*Turbo DNA polymerase (Stratagene, Heidelberg, Germany).

Alternatively, some mutations in the *sfp* gene were introduced by inverse PCR. For this purpose, oligonucleotides were used that contained the desired mutation in addition to an extra restriction site for the subsequent religation of the two ends generated by PCR (method B). For PCR, either Vent- or Herculase-Hotstart DNA polymerase (NEB, Schwalbach, Germany) was used. The generated PCR fragments were purified, digested with *Dpn*I and the appropriate restriction enzyme, and subsequently religated. XL1-Blue competent cells (Stratagene, Heidelberg, Germany) were thereafter transformed with the ligation mixture.

All constructs generated by either of the two methods were sequenced prior to heterologous expression in *E. coli*. Sequences of all primers used are listed in Table 1.

Construction of Plasmids. (A) Construction of pQE60-sfpH1. A fragment encoding Sfp's residues 1−103 was amplified by PCR from plasmid pQE60-*sfp* (*23*) using oligonucleotides 5′-catcact<u>aagctt</u>aattagctgag-3′ (restriction sites underlined) and 5′-tttt<u>aagctt</u>gctgtgaatcaaacgcaccaa-3′. The fragment was digested with *Hin*dIII and subsequently ligated into the *Hin*dIII restriction site of pQE60 (Qiagen, Hilden, Germany) to give plasmid pQE60-*sfpH1*.

(B) Construction of pQE70-sfpH2. pQE60-*sfp* served as template in a PCR with oligonucleotides 5′-aaaa<u>agcatgc</u>-cgatcggcatagatatcga-3′ and 5′-tttt<u>gatct</u>ctaggggaaatcagggtgtgc-3′ to amplify a fragment that encodes residues 104−210 of Sfp. The fragment was digested with *Sph*I and *Bgl*II and ligated into the *Sph*I and *Bgl*II sites of pQE70 to give plasmid pQE70-*sfpH2*.

Overproduction and Purification of Recombinant Proteins. E. coli BL21(λDE3) (Merck Biosciences, Schwalbach, Germany) was transformed with the mutants generated by the above-mentioned methods for the production of the Sfp-His$_6$ fusion protein mutants. An overnight culture (5 mL) of these strains in LB was inoculated into 500 mL of the same medium. In the case of all *sfp* mutants, the culture was grown at 37 °C and 300 rpm until an A_{600} of 0.15−0.2 was reached, at which the temperature was lowered to 28 °C. Expression was induced by addition of 0.1 mM IPTG (final concentration) at an A_{600} of 0.6−0.7, and the culture was allowed to grow for an additional 2 h before being harvested by centrifugation at 4500g and 4 °C. The cells were resuspended in buffer A [50 mM Hepes, 300 mM NaCl (pH 7.8)] and disrupted by three passages through a cooled French pressure cell. The resulting crude extract was centrifuged at 36000g at 4 °C for 30 min. Protein purification using Ni^{2+}-affinity chromatography was done as previously described (*24*).

Table 1: Oligonucleotides Used for Site-Directed Mutagenesis

comment	oligonucleotides 5'−3'	method
T44S	1. CTCATCGATCCCTGCTGGGAGATGTG	B
	2. GGGATCGATGAGCATCTTCTTTATG	
K75N	1. ATACGGTAACCCGTGCATCCCTGAT	B
	2. AAAGGGTTACCGTATTCCTGCGTGCT	
S89L	1. TATAGCGGCCGCTGGGTCATTGGT	B
	2. AACAGCGGCCGCTGTGCAGAATGTTGAAA	
H90A	1. TATAGCGGCCGCTGGGTCATTGGT	B
	2. AACAGCGGCCGCTGGCAGAAATGTTGAA	
H90N	1. TATAGCGGCCGCTGGGTCATTGGT	B
	2. AACAGCGGCCGCTGTTAGAAATGTTGAA	
D107N	1. GATTCACAGCCGATCGGCATTAATATCGAAAAAACGAAACCG	B
	2. CGGTTTCGTTTTTTCGATATTAATGCCGATCGGCTGTGAATC	
D107E	1. TTAAGTCAACCGATCGGCATAGAAATCGAA	B
	2. GATCGGTTGACTATCAAACGCACCAAT	
E109D	1. GATATCGATAAAACGAAACCGATCAGC	B
	2. TTTATCGATATCTATGCCGATCGGCTG	
K112A	1. CGATCGGCATAGATATTGAAAAAACGGCACCGATCAGCCTTGAG	B
	2. CTCAAGGCTGATCGGTGCCGTTTTTTCAATATCTATGCCGATCG	
E117A	1. CGAAAAAACGAAACCGATCTCGCTAGCGATCGCCAAGCGCTTC	B
	2. GAAGCGCTTGGCGATCGCTAGCGAGATCGGTTTCGTTTTTTCG	
K120A	1. CAGCCTTGAGATCGCCGCCCGCTTCTTTTCAAAAACAGAGTAC	A
	2. GTACTCTGTTTTTGAAAAGAAGCGGGCGGCGATCTCAAGGCTG	
E127A	1. CAAGCGCTTCTTTTCAAAAACAGCCTACAGCGACCTTTTAGC	A
	2. GCTAAAAGGTCGCTGTAGGCTGTTTTTGAAAAGAAGCGCTTG	
K150A	1. CTATGGTCAATGGCAGAAAGCTTTATCAAACAG	A
	2. GATAAAGCTTTCTGCCATTGACCATAGATAAAAATA	
E151S	1. GAAGAGCTCCTTTATCAAACAGGAAGGC	B
	2. AAAGGAGCTCTTCATTGACCATAGATGATA	
E151Q	1. CATCTATGGTCAATGAAACAGAGCTTTATCAAACAGGAAGGC	A
	2. GCCTTCCTGTTTGATAAAGCTCTGTTTCATTGACCATAGATG	
K155A	1. GGTCAATGAAAGAGCTTTATCGCACAGGAAGGCAAAGGC	A
	2. GCCTTTGCCTTCCTGTGCGATAAAGCTCTCTTTCATTGACC	
K155R	1. CTATGGTCAATGAAAGAGAGCTTTATCAGACAGGAAGGCAAAG	A
	2. CTTTGCCTTCCTGTCTGATAAAGCTCTCTTTCATTGACCATAG	

Those fractions containing the desired protein were pooled, brought to 10% glycerol (v/v), and stored at −80 °C.

In the case of the SfpH1 and SfpH2, the cells were resuspended in buffer IEX1 [50 mM Tris-HCl, 2 mM DTT, 1 mM EDTA (pH 7.8)] and disrupted by three passages through a cooled French pressure cell. The resulting crude extract was centrifuged at $36000g$ in 4 °C for 30 min and subsequently applied to a Hi Load 26/10 Q-Sepharose high-performance column (Amersham Biosciences, Uppsala, Sweden) previously equilibrated with IEX1 buffer at 2 mL/min. A 120 mL linear gradient to 100% IEX2 buffer (1 M NaCl in IEX1) was applied at 2 mL/min, and 3 mL fractions were taken. The fractions containing the desired SfpH1 or SfpH2 were pooled, brought to saturation with 75% (w/v) $(NH_4)_2SO_4$, and stirred at 4 °C for 1 h. Protein was subsequently collected by centrifugation at $4500g$ for 30 min. The proteins were redisolved in 10 mL of HIC1 buffer [50 mM Tris-HCl, 2 mM DTT, 1 mM EDTA, 1 M $(NH_4)_2SO_4$, pH 7.8] and applied to a Hi Load 26/10 phenyl-Sepharose high-performance column (Amersham Biosciences, Uppsala, Sweden) previously equilibrated with HIC1 buffer at 2 mL/min. A 120 mL linear gradient to 100% GFC buffer (50 mM Tris-HCl, 2 mM DTT, 1 mM EDTA) was applied at 2 mL/min, and 3 mL fractions were taken. Those fractions containing the desired SfpH1 or SfpH2 were pooled and concentrated using Vivaspin (Vivascience AG, Hannover, Germany) with a molecular mass cutoff of 5 kDa. The concentrated protein solution was applied to a Superdex75 16/60 column (Amersham Biosciences, Uppsala, Sweden) that had been equilibrated with GFC buffer. Isocratic elution was performed with GFC buffer at 1 mL/min, and 2 mL

fractions were taken. Fractions containing the SfpH1 or SfpH2 were pooled and stored at −80 °C.

The presence of the respective proteins in the fractions was detected using SDS−polyacrylamide gel electrophoresis analysis (15% Laemmli gels). TycC3-PCP, AcpS from *B. subtilis*, Sfp of *B. subtilis*, and ACP from *B. subtilis*, hereafter referred to as PCP, AcpS, Sfp, and ACP, respectively, were produced and purified as previously described (*22, 25*). Protein concentrations were determined on the basis of the calculated extinction coefficient at 280 nm: all Sfp mutants, 27220 M^{-1} cm^{-1}; SfpH1, 12330 M^{-1} cm^{-1}; SfpH2, 14890 M^{-1} cm^{-1}.

Protein Purification under Denaturing Conditions and Refolding. Because of the insolubility of Sfp mutants S89L and E151S, both proteins as well as wild-type Sfp were purified under denaturing conditions by Ni-NTA chromatography (Qiagen, Hilden, Germany), as recommended by the manufacturer, and refolded. For this purpose, harvested cells were resuspended in urea buffer B [100 mM NaH$_2$-PO$_4$, 10 mM Tris-HCl, 8 M urea (pH 8.0)], disrupted, and centrifuged as described above. A Ni-NTA column was equilibrated with urea buffer B, the crude extract was applied to the column, and unbound protein was washed off with 10 column volumes urea buffer C [100 mM NaH$_2$PO$_4$, 10 mM Tris-HCl, 8 M urea (pH 6.3)]. The protein was eluted with urea buffer D [100 mM NaH$_2$PO$_4$, 10 mM Tris-HCl, 8 M urea (pH 5.9)] and urea buffer E [100 mM NaH$_2$PO$_4$, 10 mM Tris-HCl, 8 M urea (pH 4.5)]. This pH gradient leads to protonation of histidine side chains which results in elution of the protein. The presence of the respective proteins in the fractions was detected using SDS−polyacrylamide gel

Table 2: Kinetic Constants of Sfp Mutants

Sfp mutant	K_m (mM)			k_{cat} (min^{-1})		
	PCP	hPCP	CoA	PCP	hPCP	CoA
Sfp	4.45 ± 1	26 ± 6	0.78 ± 0.2	96 ± 4	96 ± 4	98.7 ± 4
T44S	nd[a]	nd	nd	nd	nd	nd
K75N	5.8 ± 3.4	30 ± 2	1.2 ± 0.7	114 ± 11	108 ± 8	94 ± 8
S89L	78 ± 11	32 ± 7	5.5 ± 1.3	40.3 ± 10	85 ± 3.2	38.3 ± 9
H90A	5.85 ± 3	24 ± 7	2.1 ± 0.3	95.3 ± 9	87.3 ± 9	88.3 ± 4
H90N	5.2 ± 2.4	22 ± 9	1.7 ± 0.5	99 ± 5	93 ± 5	89 ± 5
D107N	11.2 ± 1.3	41 ± 3	2.3 ± 1.5	0.5−1.0	0.1−0.3	0.5−1.0
D107E	nd	nd	nd	nd	nd	nd
E109D	nd	nd	nd	nd	nd	nd
K112A	105 ± 13	510 ± 27	3.3 ± 1.5	33 ± 14	75 ± 14	68 ± 11
E117A	68 ± 17	485 ± 38	4.3 ± 0.5	39 ± 22	77 ± 18	82 ± 18
K120A	75 ± 8.2	480 ± 15	2.3 ± 0.7	56 ± 8	82 ± 3.5	77 ± 10
E127A	nd	nd	nd	nd	nd	nd
K150A	nd	nd	nd	nd	nd	nd
E151S	nd	nd	nd	nd	nd	nd
E151Q	9.5 ± 3.2	37 ± 8	1.8 ± 0.7	0.5−1.0	0.1−0.3	0.5−1.0
K155A	nd	nd	nd	nd	nd	nd
K155R	nd	nd	nd	nd	nd	nd

[a] nd: not detectable.

electrophoresis analysis (15% Laemmli gels), and the proteins were subsequently dialyzed for 4−5 h at room temperature and again for 2−3 h at 4 °C against dialysis buffer [10 mM Tris-HCl, 2 mM DTT, 100 mM NaCl (pH 7.8)] to refold the protein.

Radioassay for the Detection of Posttranslational Modification Activity (Priming Assay). The activity of Sfp and AcpS as well as the Sfp mutants was tested by a method that measures the incorporation of ^{3}H-labeled 4′-phosphopantetheine from [^{3}H]CoA into apoenzymes essentially as described earlier (*22*). Reaction mixtures (100 μL) (in duplicate) containing 50 mM Tris-HCl (pH 8.8) [75 mM MES/HCl, 250 mM NaCl (pH 6.0) in the case of Sfp and its mutants], 10 mM MgCl$_2$ (or CaCl$_2$, MnCl$_2$, CoCl$_2$, NiCl$_2$, ZnCl$_2$), 90−100 μM ACP, PCP, or hPCP, 20−100 μM CoA, 200 nM−20 μM [^{3}H]CoA (specific activity 40 Ci/mmol, 0.95 mCi/mL), and 25 nM−1 μM AcpS or Sfp were incubated at 37 °C for 30 min. Reactions were stopped by the addition of 0.8 mL of ice-cold 10% TCA (w/v) and 15 μL of BSA (25 mg/mL). Precipitated protein was collected by centrifugation at 13000 rpm and 4 °C for 15 min in a tabletop centrifuge. The pellet was washed twice with 0.8 mL of ice-cold TCA (w/v) and resuspended in 180 μL of formic acid. The resulting suspension was mixed with 3.5 mL of Rotiszint Eco Plus scintillation fluid (Roth, Karlsruhe, Germany) and counted using a 1900CA Tri-Carb liquid scintillation analyzer (Packard, Dreieich, Germany).

Kinetic Analysis. For kinetic studies, the amount of holo-carrier protein formed was determined by an HPLC method essentially as described previously (*25*).

RESULTS AND DISCUSSION

We have studied the mechanism of the Sfp/PCP recognition sites and the following phosphopantetheinylation reaction catalyzed by Sfp through mutational analysis of the CoA and PCP binding sites. In addition, we attempt to explain the broad substrate tolerance of Sfp in comparison with AcpS.

Overproduction and Purification of B. subtilis Sfp Mutants and Truncated Sfps. All Sfp mutant proteins were produced as C-terminal His$_6$ tag fusion proteins and purified by Ni^{2+}-NTA affinity chromatography. Truncated Sfps H1 and H2 were produced without tag and purified by ion-exchange, hydrophobic interaction and gel filtration chromatography (see Experimental Procedures). The yield per liter of cell culture was 10−12 mg of the Sfp mutants 2−5, 1−2 mg of the Sfp mutants 1 and 6−17 (numbering according to Table 1), and 2 mg of the truncated SfpH1 and SfpH2. All proteins had a purity of >90% as judged by SDS−PAGE. *B. subtilis* Sfp and AcpS, ACP, hPCP, and PCP were produced and purified as described previously (*22, 25*). The apo to holo ratios of purified carrier proteins as determined by either the HPLC method or the loading assay (*22, 25*) were as follows: ACP, 77−23%, PCP, 7−93%, and hPCP, 21−79%.

Posttranslational Modification of Carrier Protein Substrates by Sfp Mutants: In Vitro Studies Using ^{3}H-Labeled CoA (Priming Assay). Before the quantitative analysis, we applied a radioassay to test for the enzymatic activity of Sfp mutants regarding the modification of ACP and PCP. Because of the nature of the mutations, it was expected that some mutants completely lose their enzymatic activity. The test revealed that only 11 out of 17 Sfp mutants exhibited enzymatic activity (not shown). The mutants T44S, D107E, E109D, E127A, K150A, E151S, K155A, and K155R were inactive with PCP and ACP alike (*25*).

Biochemical Characterization of Sfp Mutants. For the determination of kinetic constants, the HPLC method (*22*) was applied. For this purpose, either CoA or the carrier protein was the variable substrate while the other one was kept above saturation. As protein substrates, PCP was chosen because it is a cognate protein substrate of Sfp and, as an ACP-like protein substrate with an increased catalytic efficiency, hPCP (*22*). For the determination of K_m and k_{cat} values, the CP concentration was varied from 1 to 125 μM with 1 mM CoA, or CoA was varied from 1 μM to 1 mM with a constant carrier protein concentration of 100 μM. Kinetic constants, which were determined through a Michaelis−Menten fit of the data sets, are summarized in Tables 2 and 3. To ensure that purification of mutants S89L and E151S under denaturing conditions had no negative effect on the catalytic properties of the enzymes, Sfp was treated the same way. However, no effect on its catalytic constants

Table 3: Catalytic Efficiencies of Sfp Mutants

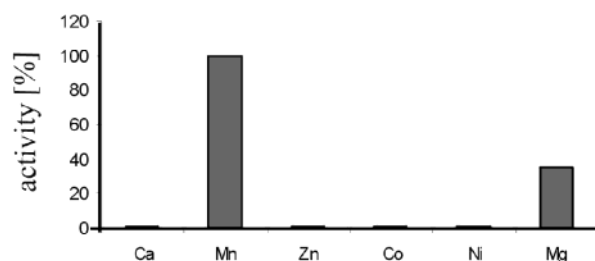| Sfp mutant	k_{cat}/K_m (min^{-1} mM^{-1})		
	PCP	hPCP	CoA
Sfp	21.6	3.7	126.5
K75N	19.6	3.6	78.3
S89L	0.52	2.6	6.7
H90A	16.3	3.6	42
H90N	19	3.7	52.4
D107N	0.04−0.08	<0.01	0.2−0.4
K112A	0.32	0.14	20.6
E117A	0.57	0.16	19
K120A	0.74	0.17	33.47
E151Q	~0.1	0.003−0.008	0.27−0.55

FIGURE 2: Influence of different metal ions on the posttranslational modification of apo-PCP by Sfp (priming assay). Reaction mixtures containing PCP (1 μM), [^{3}H]CoA, and Sfp (25 nM) were incubated for 30 min at 37 °C. The modification of apo-PCP by Sfp (gray column) is shown. Sfp modified apo-PCP in the presence of 10 mM Mg^{2+} and Mn^{2+} to the holo form.

Table 4: Kinetic Data of Mg^{2+} and Mn^{2+} Ions by Sfp

metal ion	K_m (μM)	k_{cat} (min^{-1})	k_{cat}/K_m (min^{-1} μM^{-1})
Mg^{2+}	62.5 ± 1.6	506 ± 22	8.1
Mn^{2+}	0.092 ± 0.007	229 ± 28	2491.3

was found (not shown). As apparent from Table 3, the Sfp mutants fall into three categories: the catalytic efficiency of mutants D107N, E151Q, and S89L with PCP, hPCP, and CoA is dramatically reduced compared to Sfp; however, S89L shows only 1.4-fold reduced catalytic efficiency with hPCP. Mutants K112A, E117A, and K120A exhibit reduced catalytic efficiency only with the carrier protein. Mutants K75N, H90A, and H90N show a change in catalytic efficiency only with CoA.

Influence of Different Metal Ions on the Activity of Sfp and AcpS. The fact that the reaction catalyzed by Sfp is Mg^{2+}-dependent whereas the structure of AcpS revealed the presence of a Ca^{2+} ion prompted us to investigate Sfp's activity with other divalent metal ions (Figure 2) (*19, 20*). The metal ions in question were Ca^{2+}, Mn^{2+}, Zn^{2+}, Co^{2+}, and Ni^{2+} because of their similarity to Mg^{2+}. For this purpose, reaction mixtures containing 25 nM Sfp, 100 pmol of PCP, 1 mM CoA, and 10 mM MCl$_2$ (where M is the respective metal) were incubated under the conditions described in the "priming assay" (see Experimental Procedures). Negative controls contained no Sfp or no metal ion. As expected, Sfp modified PCP in the presence of Mg^{2+} and was inactive when the metal ion was omitted. However, the addition of Mn^{2+} led to higher activity of the enzyme. In fact, the activity with Mg^{2+} is only about 40% of the activity with Mn^{2+} (Table 4). All other metal ions tested (see above) resulted in inactivation of Sfp. The same result was obtained with AcpS.
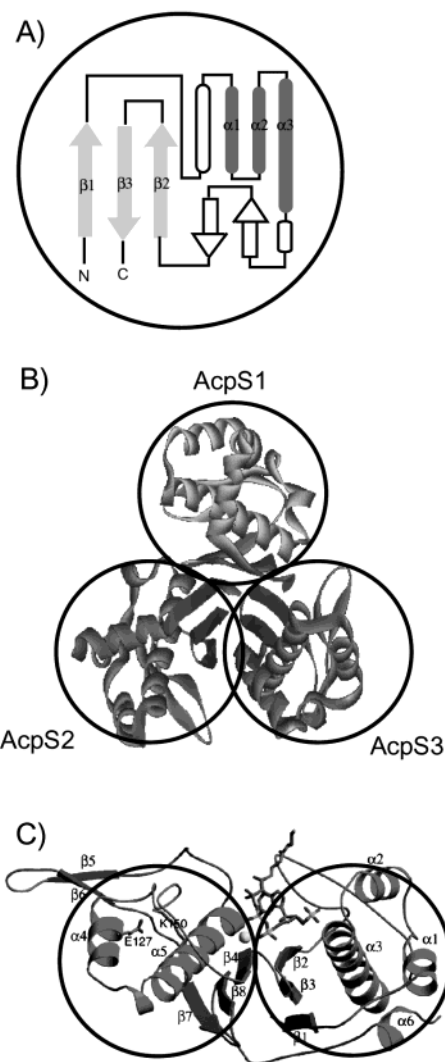

FIGURE 3: Topologies of PPTases. (A) Richardson diagram of the N-terminal folding unit of Sfp (amino acids 1−103). Dark gray represents α-helices, bright gray represents β-sheets, and white shows the difference to the minimal structure of the 4′-PPTase superfamily. (B) Ribbon representation of AcpS from *S. pneumoniae* (PDB code 1FTH) and (C) Sfp (PDB code 1QR0). In AcpS three of these folding units are assembled by ionic and hydrophobic interactions forming a trimeric complex. In Sfp two such folding units are covalently bound.

Topological Comparative Analysis of PPTases. Comparison of the secondary structures of AcpSs and Sfp in *Streptococcus pneumoniae* and *B. subtilis* (*19, 20, 26*) revealed a minimal common folding motif with one β-sheet, three α-helices, and one β-sheet (Figure 3A). Crystal structures of AcpSs indicated that in AcpSs three of these folding units (each about 120 residues) are assembled by ionic and hydrophobic interactions forming a trimeric complex (Figure 3B). In the Sfp structure, however, two such folding units are found on a single polypepide chain of about 224 residues, which leads to a pseudo-homodimeric arrangement (Figure 3C). Both conformations, the AcpS trimer as well as the Sfp pseudo-homodimer, appear to be absolutely vital for enzymatic activity and seem to be evolutionarily related (*20, 27*).

Characterization of the Truncated Variants SfpH1 and SfpH2. To address the question whether two Sfp halves would recognize each other also in solution or whether each half would dimerize or trimerize to form an active enzyme
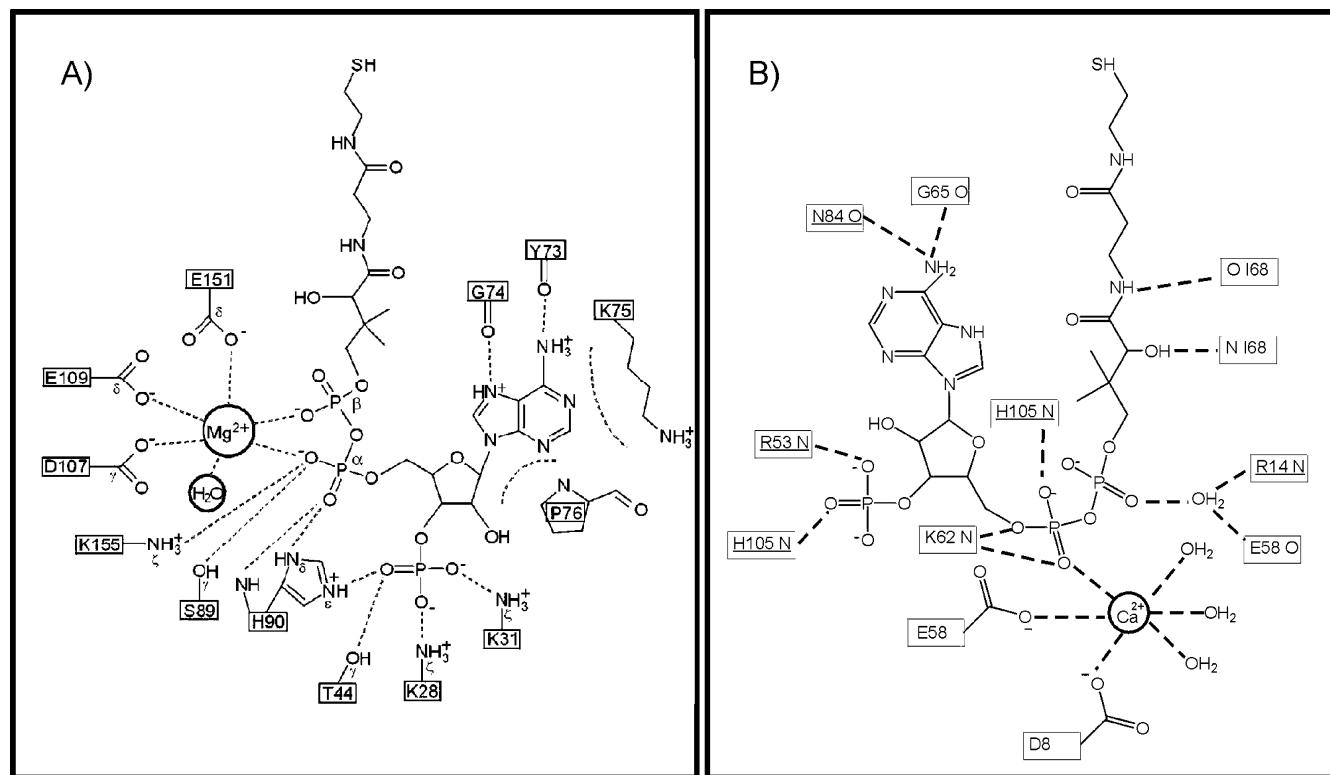
FIGURE 4: CoA binding pocket of *B. subtilis* PPTases. (A) Sfp−CoA interaction: N-terminal and C-terminal domains of Sfp interact with a Mg^{2+} ion and one molecule of CoA (*19*). (B) AcpS−CoA interaction: a molecule of CoA is coordinated by two molecules of AcpS. The residues of the second AcpS molecule are underlined. The Ca^{2+} ion is coordinated by E58 and D8 (*20*).

similar to trimeric AcpS, two truncated Sfp mutants, H1 and H2, were produced heterologously. To avoid possible interference with the dimerization, the His_6 tag was omitted. SfpH1 comprises residues 1−103 of Sfp, whereas SfpH2 consists of Sfp residues 104−210. Both proteins were tested for enzymatic activity with the substrates PCP and ACP in a qualitative radioassay that uses ^{3}H-labeled CoA (priming assay). However, neither of the mutants nor a combination of the two showed any PPTase activity with the carrier proteins tested (not shown). This indicates that neither recognition nor oligomerization of two Sfp halves, as in the case of AcpS, takes place in solution.

CoA Binding and PCP Binding Pocket of Sfp. CoA is a substrate of all PPTases. The cocrystal structure of Sfp−CoA (PBD code 1QR0) (*19*) shows that residues K28, K31, T44, K75, S89, H90, D107, E109, E151, and K155 are responsible for CoA binding (Figure 4A). Position H90, for instance, coordinates the 3′- and 5′-phosphate of CoA. Mutational analysis of H90 shows that both mutants H90A and H90N exhibit a similar catalytic efficiency with PCP (16.3 and 19 min^{-1} μM^{-1}, respectively, compared with 21.6 min^{-1} μM^{-1} for Sfp; Table 3) whereas catalytic efficiency with CoA is reduced to 50% (42 and 52.4 min^{-1} μM^{-1}, respectively, compared to 126.5 min^{-1} μM^{-1} for Sfp; Table 3). Therefore, the highly conserved H90 seems to be an important player in the coordination of CoA, albeit not essential. The mutation K75N shows a similar phenotype: catalytic efficiency with PCP remains almost unchanged, whereas with CoA it is reduced by a factor of 0.6 (Table 3). The K_m values in the case of S89L are increased 17-fold (PCP), 1.2-fold (hPCP), and 7-fold (CoA) compared with wild type. The corresponding k_{cat} values are 50% (PCP), 89% (hPCP), and 38% (CoA) of Sfp. This leads to the conclusion

that this residue is involved in binding of PCP in addition to binding of CoA. It seems that the mutation from Ser to Leu leads to steric hindrance of the Sfp−PCP interaction. Mutations T44S, D107A (*17*), D107E, E109D, E151A (*17*), E151S, K155A, and K155R inactivate the enzyme. As Figure 4B shows, all of these residues are involved in CoA binding. Thus, CoA is bound in a U-form as was shown for AcpS (Figure 4B) (*20*). By contrast, CoA is bound in a stretched form by all other CoA binding enzymes (*28*).

An important issue that was not addressed by the crystal structure is the PCP binding site of Sfp. Because of the diversity of carrier proteins, they represent a heterogeneous class of substrates for the PPTase. Sequence comparison of PCPs and ACPs alone did not reveal enough information about the carrier protein binding pocket of Sfp. First insights were gained through a superposition of the *B. subtilis* AcpS− ACP cocrystal structure with that of Sfp. The Sfp structure, however, was solved in the absence of PCP. Analysis of the AcpS−ACP structure unveiled several hydrogen bonds between α-helix 1 of AcpS and α-helix 2 of ACP (*20*). Comparison of the AcpS monomer structure with the structure of the C-terminal half of Sfp elucidates that the counterpart of AcpS's α-helix 1 (residues K13−Q22 in AcpS) is a loop between β4 and α5 (residues T111−S124) in Sfp (Figure 5). On this base, residues K112, E117, and K120 of Sfp were found to be equivalents to the AcpS residues R14, Q22, and R24 that coordinate ACP binding (Figure 5). Mutational analysis of the corresponding residues in Sfp K112A, E117A, and K120A leaves the enzyme with about 15−24-fold reduced K_m values for PCP, whereas CoA binding was only reduced about 3−6-fold (Table 2). This shows the need of these residues for PCP binding. Therefore, we hypothesize that the mode of PCP−Sfp interaction is very
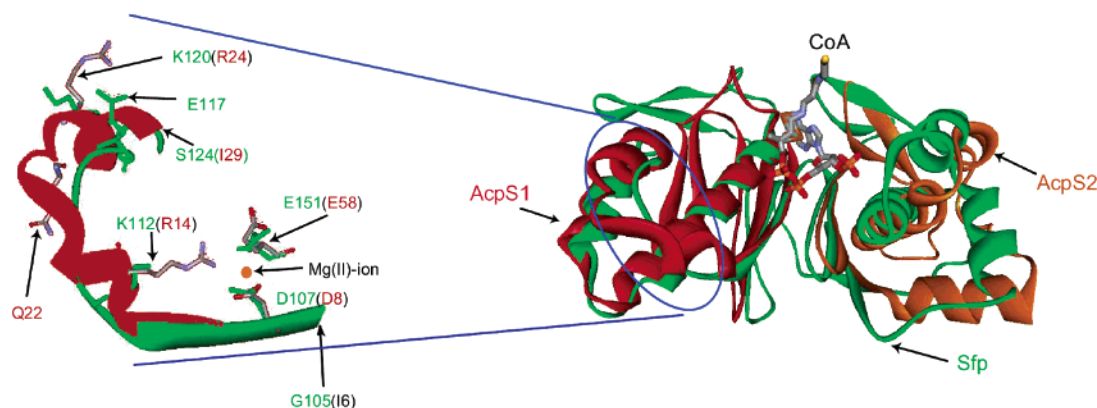
FIGURE 5: Superposition of AcpS (red and orange) on Sfp (green) from *B. subtilis*. One monomer of AcpS (PDB code 1F80) is superimposed on the N-terminal domain of Sfp and the second on the C-terminal domain of Sfp. CoA is shown in stick representation. Superposition of α-helix 1 (residues K13−Q22 in AcpS) from AcpS on the loop between β4 and α5 (residues T111−S124) in Sfp. Residues D107, E151, K112, E117, and K120 belong to Sfp (green) and residues D8, E58, R14, Q22, and R24 to AcpS (red). The Mg^{2+} ion is complexed by the carboxylate groups of D107 and E151 residues. The superposition of AcpS on Sfp was generated with the program O (*32*). The ribbon diagram was generated with WebLab ViewerPro 4.0.

similar to the interaction of helix 2 in ACP with helix 1 of AcpS in the AcpS−ACP complex (*22*) (Figure 5). Because of the loop nature of the PCP binding region of Sfp, it can be presumed, on the basis of the analysis of the three mutations which modified the loop region, that the flexibility of this region is crucial for the broad substrate tolerance of this enzyme. In contrast, AcpS provides a rigid helix for the interaction with ACP that is not easily adapted to different carrier protein structures (*20, 22*).

Reaction Mechanism. Reuter et al. previously proposed a reaction mechanism for Sfp solely based on structural data (*19*). It was postulated that the hydroxyl group of the invariant Ser in PCP is directly coordinated by the Mg^{2+} ion (Figure 6A). According to that mechanism, the oxygen atom of the hydroxyl group engages in a nucleophilic attack on the β-phosphate of CoA (step 1, Figure 6A), which results in the release of 3′,5′-ADP (step 2, Figure 6A).

From our mutational analysis and comparison of the Sfp−CoA with AcpS−CoA and AcpS−ACP complex structures, it seems more likely that PCP attacks from the side opposite the water molecule that is coordinated by Mg^{2+} (Figures 4A and 6D). In addition, the distance to the β-phosphate is about 5 Å, whereas the α-phosphate is spatially adjacent. Thus, the α-phosphate would be much more suitable for nucleophilic attack according to the mechanism proposed by Reuter et al. but is not the group which is actually attacked by the serine residue of PCP as judged by the result of this reaction (Figure 6A).

According to a second hypothesis concerning the reaction mechanism of AcpS suggested by Parris et al. (*20*), the water molecule that is coordinated by Ca^{2+} in the AcpS−CoA complex initially deprotonates a second water molecule (Figure 6B). The thus activated water molecule would subsequently deprotonate ACP's Ser-OH (step 1, Figure 6B) to enable its attack toward the β-phosphate of CoA (step 2, Figure 6B). However, such an activated water molecule would also be suitably positioned to attack the β-phosphate, which would cause CoA hydrolysis even in the absence of ACP. Neither AcpS nor Sfp have ever been shown to hydrolyze CoA. In fact, both cocrystal structures contain the intact CoA. Lastly, in the Sfp−CoA cocrystal, CoA's pyrophosphate replaces the second water molecule that was

found in the AcpS−CoA crystal structure. Since neither AcpS nor Sfp is active in the presence of Ca^{2+}, it is conceivable that the AcpS−CoA complex with Ca^{2+} is not relevant for mimicking the reaction pathway.

According to our model (Figure 6C), three negatively charged residues of Sfp, in addition to the pyrophosphate of CoA and one water molecule, are coordinated by Mg^{2+}. The Ser of PCP is localized between the carboxyl group of E151 and the β-phosphate. E151 deprotonates the hydroxyl group of PCP (step 1, Figure 6C), which in turn attacks the β-phosphate via an addition−elimination mechanism (associative phosphoryl transfer reaction) (step 2, Figure 6C), thereby releasing 3′,5′-ADP (step 3, Figure 6C). The proton of E151's carboxyl group is then transferred to D107 and further to K155, which hands it over to the oxygen of the α-phosphate (step 4, Figure 6C). Although steps 3 and 4 are described separately, they most probably occur at the same time. All of these residues are within hydrogen-bonding distance as judged from the Sfp−CoA and AcpS−CoA cocrystal structures. A similar mechanism was observed for the zinc-dependent β-lactamase from *B. cereus* and the MuT pyrophosphorylase (*29, 30*).

Mutational analysis of the highly conserved residues E151Q and D107N corroborates this theory. The mutation of the nucleophilic oxygen in E151 to the much less basic amide nitrogen results in a catalytic efficiency of Sfp that is reduced almost 1000-fold (Table 3). Similar results are obtained for the second mutation, D107N (Table 3). Here, catalytic efficiency is reduced to 0.06 and 0.3 min^{-1} μM^{-1}, respectively, for PCP and CoA. Mutations in K155 lead to total inactivation of the enzyme (see above). Likewise, a recent site-directed mutational analysis of the *Candida albicans* Lys5 PPTase revealed that E198 (corresponding to E151 in Sfp) is essential for the activation of recombinant Lys 2 α-aminoadipate reductase activity (*31*).

In our attempt to explain similarities and differences between AcpS and Sfp, we have constructed two truncated Sfps, SfpH1 and SfpH2. These two proteins correspond to the two halves of the pseudo-homodimeric Sfp. Because of the similarities between one-half of Sfp and the AcpS monomer (Figure 3), we tested whether the Sfp halves dimerize in solution or possibly imitate the trimeric organiza-
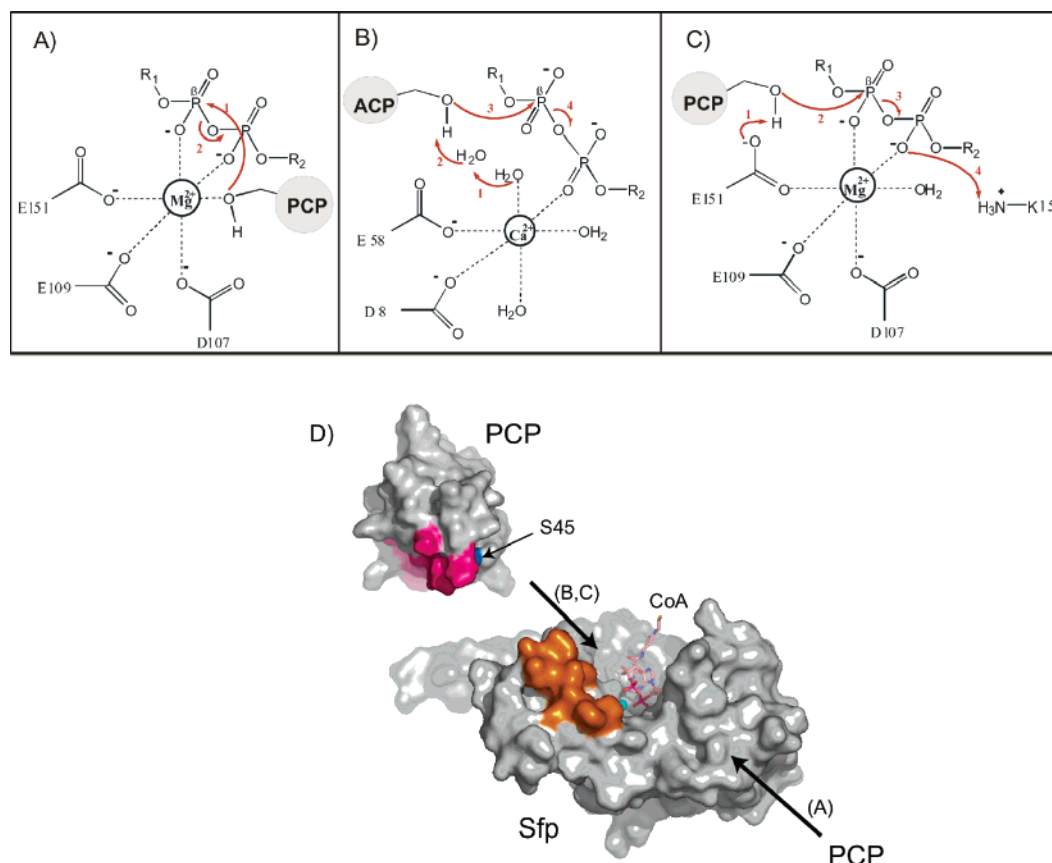
FIGURE 6: Proposed models for the priming reaction mechanism and Sfp−PCP interaction. (A) Model 1 (*19*) proposes that in the active site the hydroxyl group of Ser 45 in PCP replaces a water molecule. The hydroxyl group is coordinated and deprotonated by Mg^{2+}. Furthermore, it engages in a nucleophilic attack onto the β-phosphate of CoA (step 1). (B) Model 2 (*20*) proposes that the water molecule coordinated by the Ca^{2+} ion of AcpS first deprotonates a second water molecule (step 1); this activated water would subsequently deprotonate the hydroxyl group of Ser 36 in ACP (step 2). (C) In model 3, residue E151 deprotonates the hydroxyl group of Ser 45 in PCP which is located between the carbonyl group of E151 and the β-phosphate of CoA (step 1). The activated PCP attacks the β-phosphate via an addition−elimination mechanism (associative phosphoryl transfer reaction) (step 2), resulting in the release of 3′,5′-ADP (step 3); the proton is then transferred from E151 to D107 and further to K155, which hands it over to the oxygen of the α-phosphate (step 4), with steps 3 and 4 occurring most probably simultaneously. (D) Reuter et al. (*19*) implied for model 1 that the hydroxyl group of the invariant serine (in TycC3−PCP is S45 dark blue) in PCP attacks from the side (A) on the 5′-β-phosphate of CoA. However, the mutational analysis and comparison of the secondary structure of Sfp−CoA with AcpS−CoA and AcpS−ACP complexes indicate that PCP favors the opposite side (B, C). Orange represents the contact region of Sfp and magenta that of PCP. CoA is shown as a stick representation, and the Mg ion is in light blue. The surface representation was generated with the PyMOL Molecular Graphics System, version 0.93, by DeLano Scientific LLC, and the reaction mechanism was depicted with ChemDraw, Cambridge Soft Corp., Cambridge, MA.

tion of AcpS. However, PPTase activity was neither observed when both halves were used in the priming assay nor was there any modification of PCP or ACP with either of the halves alone.

Overall, these biochemical studies indicate that Sfp and AcpS share a number of similarities. As we could show, CoA binding and carrier protein recognition are done in a similar manner. Also, the catalytic mechanism described here is plausible for both types of PPTases. However, if the Sfp-type PPTases have evolved from the AcpS type, this has not happened by a simple gene duplication event. Sfp uses a flexible loop structure to adapt to different kinds of carrier proteins whereas AcpS uses a highly rigid helix that recognizes ACPs only. In addition, cutting Sfp in half does not produce a functionally active PPTase. A recent study has shown that bacteria can survive with a promiscuous, Sfp-type PPTase as the sole enzyme for the modification of carrier proteins from primary and secondary metabolism (*18*). Thus, it is conceivable that AcpS was the first representative of PPTases that was improved in the course of evolution to produce a highly versatile enzyme that can modify both PCPs

and ACPs and made in many organisms the AcpS-type PPTases expendable.

REFERENCES

1. Cane, D. E., and Walsh, C. T. (1999) *Chem. Biol. 6*, 319−325.
2. Hopwood, D. A. (1997) *Chem. Rev. 97*, 2465−2497.
3. Kleinkauf, H. (2000) *Biofactors 11*, 91−92.
4. Walsh, C. T., Gehring, A. M., Weinreb, P. H., Luis, E. N., and Flugel, R. S. (1997) *Curr. Opin. Chem. Biol. 1*, 309−315.
5. Van Wageningen, A., Kirkpatrick, P., Williams, D., Harris, B., Kershaw, J., Lennard, N., Jones, M., Jones, S., and Solenberg, P. (1998) *Chem. Biol. 5*, 155−162.
6. Weber, G., Schorgendorfer, K., Schneider-Scherzer, E., and Leitner, E. (1994) *Curr. Genet. 26*, 120−125.
7. Lambalot, R. H., Gehring, A. M., Flugel, R. S., Zuber, P., LaCelle, M., Marahiel, M. A., Reid, R., Khosla, C., and Walsh, C. T. (1996) *Chem. Biol. 3*, 923−936.

8. Quadri, L. E., Sello, J., Keating, T. A., Weinreb, P. H., and Walsh, C. T. (1998) *Chem. Biol. 5*, 631−645.

9. Marahiel, M. A., Stachelhaus, T., and Mootz, H. D. (1997) *Chem. Rev. 97*, 2651−2674.

10. Borchert, S., Stachelhaus, T., and Marahiel, M. A. (1994) *J. Bacteriol. 176*, 2458−2462.

11. Mootz, H. D., Schörgendorfer, K., and Marahiel, M. A. (2002) *FEMS Microbiol. Lett. 213*, 51−57.

12. Kiriukhin, M. Y., and Neuhaus, F. C. (2001) *J. Bacteriol. 183*, 2051−2058.

13. Ritsema, T., Geiger, O., van Dillewijn, P., Lugtenberg, B. J. J., and Spaink, H. P. (1994) *J. Bacteriol. 176*, 7740−7743.

14. Silakowski, B., Schairer, H. U., Ehret, H., Kunze, B., Weinig, S., Nordsiek, G., Brandt, P., Blocker, H., Hofle, G., Beyer, S., and Muller, R. (1999) *J. Biol. Chem. 274*, 37391−37399.

15. Fichtlscherer, F., Wellein, C., Mittag, M., and Schweizer, E. (2000) *Eur. J. Biochem. 267*, 2666−2671.

16. Lambalot, R. H., and Walsh, C. T. (1997) *Methods Enzymol. 279*, 254−262.

17. Quadri, L. E., Weinreb, P. H., Lei, M., Nakano, M. M., Zuber, P., and Walsh, C. T. (1998) *Biochemistry 37*, 1585−1595.

18. Finking, R., Solsbacher, J., Konz, D., Schobert, M., Schäfer, A., Jahn, D., and Marahiel, M. A. (2002) *J. Biol. Chem. 277*, 50293−50302.

19. Reuter, K., Mofid, M. R., Marahiel, M. A., and Ficner, R. (1999) *EMBO J. 18*, 6823−6831.

20. Parris, K. D., Lin, L., Tam, A., Mathew, R., Hixon, J., Stahl, M., Fritz, C. C., Seehra, J., and Somers, W. S. (2000) *Struct. Folding Des. 8*, 883−895.

21. Sambrook, J., Fritsch, E. F., and Maniatis, T. (1989) *Molecular Cloning: A Laboratory Manual*, Cold Spring Harbor Laboratory Press, Cold Spring Harbor, NY.

22. Mofid, M. R., Finking, R., and Marahiel, M. A. (2002) *J. Biol. Chem. 277*, 17023−17031.

23. Mofid, M. R., Marahiel, M. A., Ficner, R., and Reuter, K. (1999) *Acta Crystallogr., Sect. D: Biol. Crystallogr. 55*, 1098−1100.

24. Linne, U., Stein, D. B., Mootz, H. D., and Marahiel, M. A. (2003) *Biochemistry 42*, 5114−5124.

25. Mootz, H. D., Finking, R., and Marahiel, M. A. (2001) *J. Biol. Chem. 276*, 37289−37298.

26. Chirgadze, N. Y., Briggs, S. L., McAllister, K. A., Fischl, A. S., and Zhao, G. (2000) *EMBO J. 19*, 5281−5287.

27. Nakano, M. M., Corbell, N., Besson, J., and Zuber, P. (1992) *Mol. Gen. Genet. 232*, 313−321.

28. Modis, Y., and Wierenga, R. (1998) *Structure 6*, 1345−1350.

29. Fabiane, S. M., Sohi, M. K., Wan, T., Payne, D. J., Bateson, J. H., Mitchell, T., and Sutton, B. J. (1998) *Biochemistry 37*, 12404−12411.

30. Lin, J., Abeygunawardana, C., Frick, D. N., Bessman, M. J., and Mildvan, A. S. (1997) *Biochemistry 36*, 1199−1211.

31. Guo, S., and Bhattacharjee, J. K. (2003) *FEMS Microbiol. Lett. 224*, 261−267.

32. Jones, T., Zou, J. Y., Cowan, S. W., and Kjeldgaard (1991) *Acta Crystallogr. A 47*, 110−119.